
The morphology of urban land use

M Batty, P A Longley

Department of Town Planning, University of Wales at Cardiff, PO Box 906, Cardiff CF1 3YN, Wales
Received 20 June 1988

Abstract. The irregularity of land uses and land parcels which constitute the morphology of a small English town is measured. Form is described by the digitised perimeters and areas of land-use parcels, and various methods are introduced which relate area to perimeter, and perimeter to scale, enabling the degree of irregularity to be assessed by means of the concept of fractal dimension. A theoretical exposition of scale and dimension leads to the definition of methods for relating area and scale to perimeter, which are then tested using land-use data for the town of Swindon, Wiltshire. Residential, commercial-industrial, educational, transport, and open space constitute the range of land uses defined, and three approaches based on area-perimeter, aggregated perimeter-scale, and individual perimeter-scale regressions are tested. The methods tested, although well established, are demonstrably inadequate, but some consistency in gauging the range of irregularity over the set of land uses is presented. It is suggested that future work be orientated towards more disaggregated measures of land-parcel irregularity.

Introduction

During the last twenty years, analysis of the regularities in the form of cities has been largely based on models which identify activities which scale with one another. Such scaling relations are central to social physics; they are manifest in the way movement between places is attenuated or scaled inversely with distance, and the way in which different sized places are clustered in the urban hierarchy. Distance, size, and frequency are embodied in spatial interaction models of movement and in central place theory, in which city size is structured around the idea of a rank-size rule.

Hitherto, there has been little emphasis on the meaning of the scale coefficients associated with such models. In gravitational models, for example, departures from the inverse square law are defined away as behavioural effects, distinct from the physical constraints of space. In the last ten years, however, a powerful new geometry has emerged. This is not only able to interpret scaling relations in a new light and explain differences from theoretical postulates; it is able to demonstrate how the regularity posed by Euclidean geometry, with its emphasis on simple dimensions, can be generalised to embrace the kinds of irregularities empirically associated both with natural and with artificial realities. Fractal geometry, as it has been termed by its popularist Mandelbrot (1983), is able to explain many types of irregular form which have hitherto resisted scientific classification and explanation. This geometry enables 'order' to be extracted from what has always been considered 'chaos', and it has heralded a new dawn for the age-old study of theories of form.

There are three central constructs to fractal geometry. In essence, the geometry concerns relationships based on scaling, but with the characteristic that such relationships are *invariant to scale*: that is, relationships hold over several orders of magnitude. The consequence of this first idea is a second one which suggests that the form of the objects in question is similar over these orders of magnitude. In short, such objects appear the same when viewed at different scales, typical examples being rough terrain, branching structures such as trees, cloud formations, and so on. Fractal objects such as these are called *self-similar*. The third concept is the

most powerful and involves dimension. Euclidean geometry deals with the integral dimensions: 1, 2, 3, and upwards to the higher dimensions. Fractal geometry is based on noninteger, 'fractional', or as it is now referred to, *fractal dimension*. The basis on which an object is fractal or not is its irregularity over scale, and if the object is self-similar, its form can be captured in the single measure of its fractal dimension. If such a dimension can be computed with confidence, the objects in question must clearly manifest self-similarity and scale invariance, albeit usually in a statistical sense.

The simplest fractals to visualise are those whose dimensions lie between 1 and 2. The best example is that of a natural boundary such as a coastline which is more irregular than a straight line of dimension 1, but is clearly less than the area of a plane which has dimension 2. As such boundaries become more tortuous, the fractal dimension increases until the curve in question twists and turns to fill the space available. There are many conundrums in measuring such fractal curves, for it can easily be shown that the length of such curves depends upon the scale and sophistication of the measuring device, although the area enclosed by such curves is always finite. Natural phenomena such as coastlines and man-made boundaries such as frontiers are both fractals (Richardson, 1961). It is clear that a preliminary approach to measuring the extent and irregularity of urban areas must begin with an assessment of the extent to which the boundaries defining such areas are fractal. In this paper, we will extend our earlier work in measuring such boundaries (Batty and Longley, 1987a; 1987b) to different urban land uses constituting a medium sized English town, Swindon, Wiltshire which had a population of 125 000 in 1981. This paper will also embrace an attempt to classify various land uses on the basis of their fractal dimensions.

There have been many attempts in several disciplines to use fractal geometry to measure morphologies by defining edges which can be treated as boundaries. In fine particle science, there is a stream of work based on measuring the irregularity of two-dimensional outlines (Kaye, 1986). Much work exists in defining the fractal dimensions of coastlines (Kaproff, 1986) and terrain (Mark and Aronson, 1984), in the geometry of fracture (Aviles et al, 1987), and in cartographic line generalisation (Muller, 1987). This is apart from the enormous literature that now exists in the physics of phase transitions, meteorology, the mathematics of iterated functions, and in computer graphics. We have referenced only those areas which involve the definition and measurement of identifiable boundaries in the plane, and the literature cited is the latest we have come across in a long line of related work. Interested readers are also referred to the review article by Goodchild and Mark (1987) for a recent survey of applications in spatial analysis.

Methods for determining the fractal dimension, and hence the irregularity of curves, are comparatively straightforward. Richardson (1961) first demonstrated the usual method, which consists of measuring the length of a curve at different scales, and finding the least squares fit of length to scale from which the dimension is an immediate consequence. However, the method is sensitive to the way length is measured, and to the number of scales over which the relationship is likely to hold. We have demonstrated variations and problems in this method in earlier papers (Batty and Longley, 1987a; 1987b); here we will extend these ideas, but the main purpose of this paper is to explore the extent to which we can associate different boundaries with different areas, in this case of land uses, based on their fractal dimensions. An immediate problem which will be raised is the fact that most land uses share the same boundaries with other land uses; in a system of contiguous areas like a town, the boundary to each use will always consist of parts

of the boundary of other uses. The convoluted nature of every boundary poses severe conceptual problems which we will raise, if not resolve, for the first time here.

We will begin by providing a consistent summary of the mathematics of scale and dimension involving the line and the plane. We will then present two models of scale dependence, and four methods or algorithms for extracting fractal dimensions from various boundary data. The application of these methods to land-use boundaries in Swindon is then presented beginning with a description of the characteristics of the urban area in question. Fractal dimensions based on area-perimeter relations across scales are then estimated, and these same dimensions are then derived by examining scale changes within the digital representation of the perimeters themselves. Last, individual dimensions of each of the land-use parcels are derived, and interpretations are made as to the extent to which land uses can be classified on the basis of their fractal dimensions. The analysis presented is inconclusive, but it is clear that careful measurement is required in such applications. The sensitivity of the analysis here to measurement differences casts considerable doubt on many of the applications presented so far in a variety of fields. Directions for further research are then indicated.

The mathematics of scale and dimension

In Euclidean geometry, the measure of size in a given dimension will scale directly with the measure in another (for example, adjacent) dimension; this scaling will be some product of the dimensions themselves. Consider area A and volume V based on two dimensions and three dimensions, respectively. Area has a size calculated as the square of the line measure P , that is P^2 , and volume has a size P^3 . If it is required to derive area from volume, it is clear that this can be done as $A \propto V^{2/3}$. In the same way, if it is required to derive the base line P , which we will henceforth call perimeter, from area A , the relation is

$$P \propto A^{1/2}. \quad (1)$$

All relationships such as those implied by equation (1) show that size in one dimension can be scaled directly if one knows the dimension of the object in a higher or lower dimension. For example, if $A = \pi r^2$, the area of a circle with radius r , $P \propto \pi r$, and so on for a variety of regular forms. These types of relation appear widely in the natural sciences where they form an essential part of the study of relative growth, or allometry (Gould, 1966). If the relationship between line and area is as postulated in equation (1), this is the condition of isometry. If the power of A were greater than $\frac{1}{2}$, this would be positive allometry, if less, this would be negative allometry.

Let us now define the area at a given scale n as A_n . If area is regarded as a measuring device for the perimeter, now called P_n , when the scale is increased to $n+1$, it is clear that

$$\frac{P_{n+1}}{P_n} > \left(\frac{A_{n+1}}{A_n} \right)^{1/2}, \quad (2)$$

because more and more scaled detail about the boundary will be picked up. In fact, the conundrum emerges that, in the limit as $n \rightarrow \infty$, the ratio of areas in equation (2) will converge, but the ratio of the perimeters will continue to increase. From equation (1) it is clear that, to derive P from A , area must be rescaled by a parameter which is greater than 1 but less than 2. That is

$$P \propto (A^{1/2})^D = A^{D/2}, \quad (3)$$

where $1 < D < 2$. If $D = 2$, then perimeter would scale up as area, which would

imply that area be defined as a space-filling curve, a physically impossible realisation for the kinds of systems dealt with here. If $D = 1$, perimeter would not scale more than the basic unit of measurement which would imply that no scale effects were present as area increased. The coefficient D is known as the Hausdorff-Besicovitch or fractal dimension (Mandelbrot, 1983). In this context it serves as an empirical measure of how much the curve in question departs from a straight line, thus indicating how 'crinkled' or tortuous the boundary across the space is. The relation in equation (3) is known as the area-perimeter relation and it clearly implies a way of estimating the value of D (Lovejoy, 1982).

There is another way of showing how perimeter is related to the scale of measurement. Consider a scale defined by a unit Δx_n , where this is the basic unit used to define the perimeter P_n . When Δx_n is used to define the perimeter, it yields N_n chords such that $P_n = \Delta x_n N_n$. Assume that the scale is now halved, so that $\Delta x_{n+1} = \frac{1}{2}\Delta x_n$. This scale then yields N_{n+1} chords, but, as finer detail is picked up, $P_{n+1} > P_n$, which implies that

$$\frac{N_{n+1}}{N_n} > 2, \quad \text{while} \quad \frac{\Delta x_n}{\Delta x_{n+1}} = 2. \quad (4)$$

Equation (4) shows that halving the scale yields more than twice the number of chords or line segments.

To derive N_{n+1} , hence P_{n+1} , from Δx_{n+1} , we can write equation (4) as

$$\frac{N_{n+1}}{N_n} = \left(\frac{\Delta x_n}{\Delta x_{n+1}} \right)^D, \quad (5)$$

where $D > 1$ in the given case. Equation (5) can also be written as

$$N_{n+1} = \left(\frac{P_n}{\Delta x_{n+1}} \right)^D, \quad (6)$$

but, as P_n can be regarded as a base-level constant (a previous estimate of the perimeter), equation (6) can be simplified to

$$N_{n+1} = \lambda \Delta x_{n+1}^{-D}. \quad (7)$$

The perimeter P_{n+1} is now calculated from equation (7) as

$$\begin{aligned} P_{n+1} &= \Delta x_{n+1} N_{n+1} = \lambda \Delta x_{n+1} \Delta x_{n+1}^{-D} \\ &= \lambda \Delta x_{n+1}^{1-D}. \end{aligned} \quad (8)$$

More generally, the relation between any perimeter P and its scale Δx can be written as

$$P \propto \Delta x^{1-D}. \quad (9)$$

We thus have two relationships for P , one in terms of area, as in equation (3), and one in terms of scale, as in equation (9). Combining these gives

$$P \propto A^{D/2} \propto \Delta x^{1-D}. \quad (10)$$

It is tempting to try to equate these by considering how A relates to the scale, Δx . However, it is not possible to do this in general, for it is only meaningful in special cases where the geometry is known or assumed.

Besides the area-perimeter, and perimeter-scale relations, there is a third which could be used to estimate the fractal dimension, D . This is the number-area rule, known as Korcak's law (Mandelbrot, 1977; 1983). It relates the number of or

fraction of areas, $F(A)$, with an area greater than A , to the area itself as

$$F(A) \propto A^{-D/2}. \quad (11)$$

We will not use equation (11) in the sequel for it requires a much larger number of areas (in this case, land-use parcels) than the level of resolution of the example we have chosen permits. Nevertheless, there may be circumstances amongst the kinds of applications described here where it might be useful.

Determining irregularity through the estimation of fractal dimension

The area-perimeter and perimeter-scale relations in equations (3) and (9), respectively, are both power laws, the parameters of which can be estimated by means of least squares regression on their logarithmic transformations. However, the data for these estimations are quite different. For the area-perimeter relation, it would in theory be possible to measure the area and perimeter of an irregular object at different scales and perform the regression on these measurements; but the relation is more suited to estimation with a series of areas and perimeters associated with a set of objects, all of different sizes. If the relationship holds over many scales, more scaling detail will be picked up in larger objects than in smaller ones. In contrast, the perimeter-scale relation is best estimated by calculating perimeter lengths at different scales for the same object. Later in the paper, we will explore the consequences of these two methods and note some of the conceptual difficulties resulting from their comparison. In the rest of this section, however, we will concern ourselves solely with their estimation and with techniques for measuring the effects of scale.

First, we will write the area-perimeter relation in equation (3) as

$$P = \phi A^{f(D)} \quad (12)$$

where ϕ is a constant of proportionality and $f(D)$ is some power function involving the fractal dimension D , in this case $f(D) = \frac{1}{2}D$. Taking logs of equation (12) gives

$$\ln P = \ln \phi + f(D) \ln A, \quad (13)$$

where, in the case of equation (3), $\ln \phi$ is the intercept and $f(D) = \frac{1}{2}D$ is the slope of the regression line of the log of perimeter on the log of area. Clearly, the slope $f(D)$ can take different functional forms from which D can always be derived, given an estimate of the slope. The perimeter-scale relation in equation (9) can also be generalised as

$$P = \lambda \Delta x^{g(D)}, \quad (14)$$

where λ is a constant of proportionality and $g(D)$ a power function, which in terms of equation (9) is $g(D) = 1 - D$. Taking logs of equation (14) gives

$$\ln P = \ln \lambda + g(D) \ln \Delta x, \quad (15)$$

where $\ln \lambda$ is the intercept and $g(D) = 1 - D$ is the slope of the regression of the log of perimeter on the log of scale.

The conventional fractal model based on the use of equation (3) in equation (13) and equation (9) in equation (15), has a linear form, which implies that D is scale-invariant. However, in some contexts, it can be hypothesised that dimension itself might vary with scale or area and, in this case, the linear form would be more complex. We have used a second model based on the notion that fractal dimension does vary systematically with scale to model the perimeter-scale relations for the boundaries of urban development in the town of Cardiff (Batty and Longley, 1987b).

These models will also be tested here. In the case of the area-perimeter relation, the fractal dimension D can be hypothesised as $f(D) = \frac{1}{2}(c + dA^d)$ which when used in equation (13) gives

$$\ln P = \ln \phi + \frac{1}{2}c \ln A + \frac{1}{2}dA^d \ln A. \quad (16)$$

In equation (16), the coefficient $\frac{1}{2}c$ has an analogous role to $\frac{1}{2}D$ in equation (3) as applied to equation (13). The third term on the right-hand side of equation (16) is a dispersion factor which measures the nonlinearity of the area-perimeter relation. It is also clear that, as $d \rightarrow 0$, $c \rightarrow D$ and equation (16) collapses back to the logarithmic transformation of equation (3).

For the perimeter-scale relation, the hypothesis becomes $g(D) = 1 - D = a + b\Delta x$, where D is a linear function of the scale Δx . Using this in equation (15) gives

$$\ln P = \ln \lambda + a \ln \Delta x + b \Delta x \ln \Delta x. \quad (17)$$

As $b \rightarrow 0$, $(1 - a) \rightarrow D$ and equation (17) collapses back to the logarithmic transformation of equation (9) in equation (15). The third term on the right-hand side of equation (17) is a dispersion factor, again measuring the nonlinearity of the perimeter-scale relation, and thus acting as a kind of weighted entropy modulating the effect of the fractal dimension. In some contexts involving research into the stability of dimensions across scales, it has been postulated that the data are best fitted by a multifractal model in which several distinct regression lines can be discerned. In short, various ranges of scale are reflected by different dimensions (Kaye et al, 1985; Orford and Whalley, 1983). The model implied by equations (16) and (17) is the logical consequence of this multifractal specification (Suzuki, 1984). In the rest of the paper, this model based on the systematic variation of dimension with area or scale will be referred to as the *modified* model in contrast to the *conventional* model of equations (3) and (9) where dimension is scale-invariant.

Estimating D for the two models from the area-perimeter relations in equations (13) and (16) is straightforward. For each land parcel, the area and perimeter can be easily measured and form the dependent and independent variables, respectively. The number of parcels in the study obviously affects the fit of the regression, and it may be necessary to identify and exclude outliers. However, the variation in scale within the observations forming the data set is only influenced by the prior selection of land parcels, not by any peculiarity of the area-perimeter measurement.

In contrast, the perimeter-scale relations depend upon the choice of scale and the measurement of the perimeter associated with that scale for each individual object. In this case, we will form aggregate perimeters from more than one land parcel in the first instance. We have used four methods which enable these measurements to be made. These methods are examined in detail elsewhere (Longley and Batty, 1986), but they will be summarised here. The most accurate and time-consuming method involves traversing the perimeter of the object at different scales by 'walking' a pair of dividers set at an appropriate scale around the perimeter, thus enabling the perimeter to be derived as a function of the number of chords generated, N_n , and the divider length, Δx_n , used; that is, $P_n = \Delta x_n N_n$. This method was first used by Richardson (1961) to derive the log-log plots of perimeter versus scale, as implied by equation (15); these graphs have been subsequently called 'Richardson plots' by Kaye (1978) who also refers to the method as the *structured walk*. Richardson used a literal, hence manual, version of this method but here we are able to simulate the walk with a computer algorithm similar to that suggested by Shelby et al (1982).

The structured walk is time-consuming because it involves a trigonometric interpolation between the digitised points on the perimeter, to determine the location of the start and end points of each chord which approximate the perimeter at the given scale. To reduce the computer time required, a second method suggested by Kaye and Clark (1985), which they refer to as the *equipaced polygon* method, involves computing the approximation to the perimeter from chords based on successive sequences of every second, or third, or fourth (and so on) point defining the base-level perimeter. The chords at any level of aggregation are thus not equal to one another, but the aggregation is very quick. It is argued that this method enables deep fissures as well as heavily digitised sections of the base-level perimeter to be more clearly detected than by the structured walk method, since it takes account of the original digitisation of points which are rarely equally spaced.

A third method which we call the *hybrid walk* method was first suggested by Clark (1986) as a compromise between the time-consuming structured walk and the quicker equipaced polygon method. As in the structured walk method, a divider length or scale, Δx , is fixed, but instead of interpolation of each chord onto the original base-level perimeter, the chord is fixed by approximating its end point as the nearest point on the original curve.

The fourth and final method is based on approximating the perimeter by means of a grid of cells whose spacing is set at different scales over the range of scales adopted. At each scale, the perimeter is calculated by counting the number of cells which are astride the original curve, and it is thus called the *cell count* method (Goodchild, 1980). This is the only method in which scale aggregation is consistent over the entire area and perimeter of the object. In essence, it approximates the original curve by rasterised images at different scales, whereas the other three methods use the original curve to fix the scale at different levels. The cell count method is thus the least accurate with respect to the resolution of the original object, but is the most consistent with respect to objective scale aggregation.

There are three additional features characterising the use of these methods. First, with N points defining the base-level curve, the perimeter values obtained are not independent of their starting point. Thus, each method has been applied by starting at each of the N digitised points and forming an average perimeter value from the N perimeter estimates obtained. For boundaries with several thousand points, a method such as the structured walk can take several hours of cpu time on a VAX 11/780 machine if an average perimeter is required for each scale. As we have had sole access to such a machine for several days at a time this has not constituted a problem; further details of these aspects of this kind of simulation are given in Longley and Batty (1986).

Second, from each starting point, none of the methods will close exactly on the first and last points in the base-level curve. A fraction of the chord length will usually remain, and thus, in all applications, we have added these fractions to the perimeter values.

Third, the range of aggregations used varies from scales which are fixed at the average chord length of digitised base-level data up to the value of the maximum spanning distance between any separate sets of points on the original object, this maximum being known as Feret's diameter (Kaye, 1978). Within this range, with a given number of aggregations to perform, the scales are determined in geometric progression so that they will be equally spaced with respect to the logarithmic regression.

Applications to urban land use: the area-perimeter relations

Swindon, Wiltshire, the town chosen for analysis, is located in south central England about 70 miles west of London. The town is quite compact and not affected in its form by any rapidly growing nearby towns. It has a reasonably buoyant economy which in the 1960s was a result of its designation as an expanded town, taking overspill population from Greater London. More recently, its favoured location in a rapidly expanding area of southern England has led to the location of new service and high-technology industries in and around the town itself. Figure 1 shows land use in the town in 1981. It is clear that, as the town has grown, it has absorbed villages in its immediate periphery. Figure 1 was compiled as a fairly aggregated land-use map from diverse data sources: remotely sensed data and local authority map records used by Rickaby (1987) as part of his studies into the energy requirements of small towns.

The five land uses—residential, commercial-industrial, educational, transport, and open space—shown in figure 1 constitute the basic data for this study. The map was digitised with the Map Manager software (Bracken et al, 1987) and the land parcels were extracted in polygon form by means of conventional digital cartographic techniques in software developed by the authors. Figure 2 shows the polygons which constitute the land parcels; they are drawn to scale and classified according to the five land uses, but they are not arranged in any particular order. When one observes how these parcels fit together to form the overall map, the conundrum raised earlier relating to contiguous boundaries between different uses is immediately apparent. For example, the largest land parcel of all is part of the set of residential land uses shown in figure 2. In one sense, this parcel can be considered as the skeleton of the entire town, but it is clear that about half its

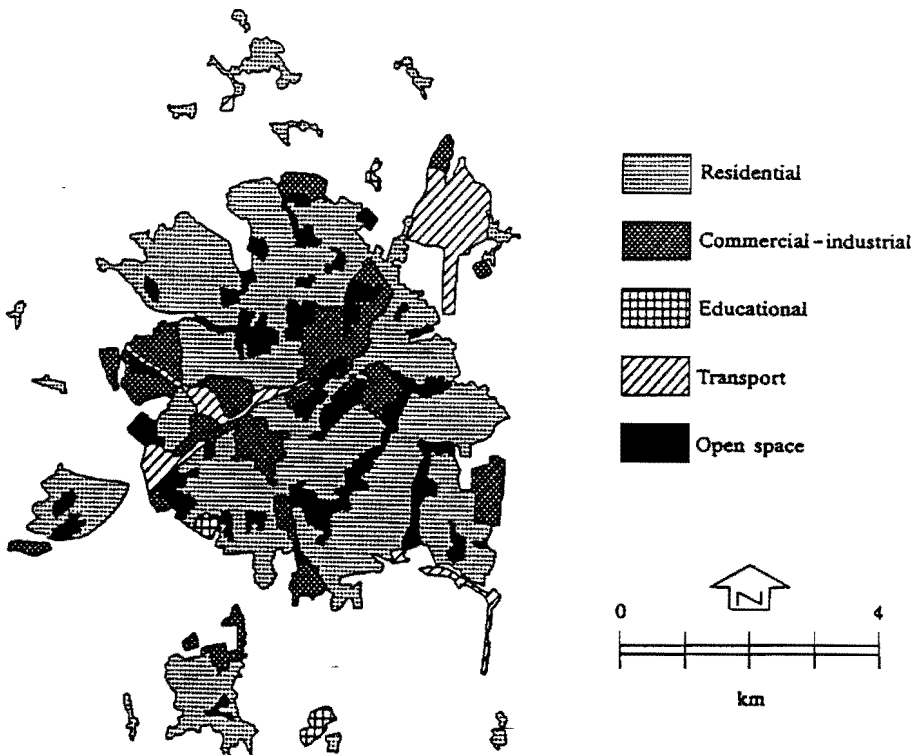


Figure 1. Urban land use in Swindon, 1981.

boundary is common with other land uses; this raises the conceptual difficulty of making comparisons of the irregularity and form of this boundary with that of adjacent land uses. For the moment, we will assume that the different parcels can be treated separately, and we will pursue the estimation in this manner before commenting further on the problem later in this paper.

Some characteristics of the digital representation of the five land uses are presented in table 1. There is considerable variation in the set of land uses and it is clear that no generalisations can be made about educational land use which comprises only three parcels; and there are limits to how far one can make inferences about the transport land use which comprises only six parcels. However, an examination of the average chord length of these data, which ranges from 0.7266 to 0.8375 base-level units, indicates that the base-level digitisation is fairly independent of land-use type. The number of digitised points given in table 1 for each land use and for the total involves the double counting of common boundaries referred to above, in that the points which are common to any pair of land uses are included in each land use.

Of the 6059 points which constitute the total number of points in each of the distinct land uses, there are only 2335 points which are not common to adjacent land-use boundaries. The remaining 3724 points which are common to various pairs of land uses are in fact counted twice (for each land use in each pair) and thus there are 1862 points which are common in the data set. In total, there are 4197 distinct points in the set, 43% of these being common to adjacent land uses. In terms of the individual uses, 51% of the points defining the residential parcels are common to other uses, whereas over 90% of the points referring to open space are part of the boundaries of other land uses. These percentages, shown in table 1, give some indication of the position of the land uses within the town. For example,

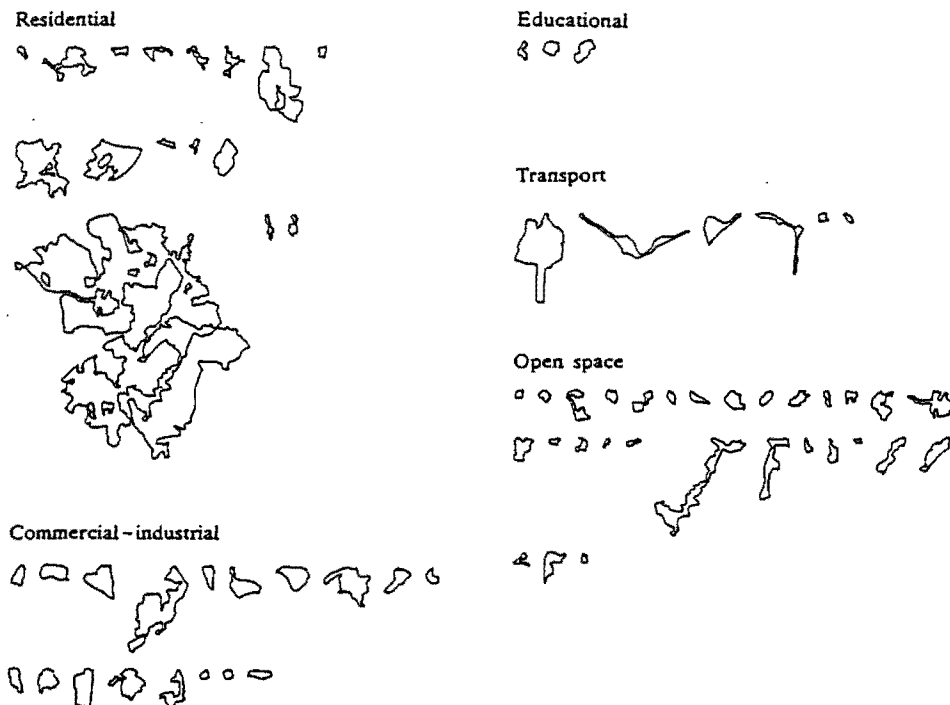


Figure 2. Land parcels separated into distinct land uses.

most of the open space is enclosed within the town itself, not on its edge, whereas educational land use is mainly on the town's edge. In table 1, the perimeter length refers to the sum of all the perimeters relating to a given land use and the Feret diameter represents the maximum spanning distance found amongst the parcels of any given land use. It is clear from this and from figure 2 that there is some considerable variation among land-use parcels with respect to size.

We are now in a position to estimate the first set of fractal dimensions based on the area-perimeter relation. In figure 3, the log-log plots of perimeter against area are presented as scatter diagrams for each of the five sets of land uses in turn, and then for all five land uses making up the seventy-two land parcels in the town. These plots demonstrate strong relationships between perimeter and area, and it is difficult to detect any significant nonlinearity in their form. To these data we have fitted the conventional model based on using equation (3) in equation (13), which we can restate as

$$\ln P = \ln \phi_1 + \frac{1}{2} D \ln A, \quad (18)$$

and the modified model given earlier in equation (16), which we will also repeat for convenience as

$$\ln P = \ln \phi_2 + \frac{1}{2} c \ln A + \frac{1}{2} d A^{1/2} \ln A. \quad (19)$$

Note that we now distinguish the intercept terms in equations (18) and (19) as ϕ_1 and ϕ_2 , respectively.

The results of these regressions are presented in table 2. With the exception of educational land use where there are only three observations, the adjusted R^2 (correlation) statistics for both sets of models are acceptable. There are no obvious outliers, for example, whose removal might improve these statistics. The modified model gives a slight improvement over the conventional one, but this is not significant. The fractal dimensions in the conventional model are as postulated, that is, $1 < D < 2$, with the exception of the educational land use which we must exclude from serious analysis. Interpretations of the parameter c in the modified model are problematic because of the size of d . As $d \rightarrow 0$, it is hypothesised that $c \rightarrow D$, but none of these results show any meaning in these terms in contrast to some previous work of the authors (Batty and Longley, 1987b). The conventional model is the only one acceptable here and excluding education, the analysis suggests that the commercial-industrial ($D \sim 1.47$) and transport land uses ($D \sim 1.44$) have more tortuous boundaries than those of residential ($D \sim 1.33$) and open space ($D \sim 1.24$). The dimension associated with all the land uses ($D \sim 1.29$) is clearly an average. All these results are consistent with other estimates from aerial data

Table 1. Characteristics of digitised urban land use in Swindon.

Land use	Number of parcels	Number of digitised points, N	Number of common points	Percentage of common points
Residential	16	2989	1534	51.4
Commercial-industrial	18	1030	626	60.8
Educational	3	109	17	15.6
Transport	6	510	261	51.2
Open space	29	1421	1286	90.5
All land uses	72	6059	3724	61.5

produced by applications of the area-perimeter method (Lovejoy, 1982; Woronow, 1981) but the correlations are not as good. Nevertheless this provides a backcloth and comparison to the perimeter-scale analyses which now follow.

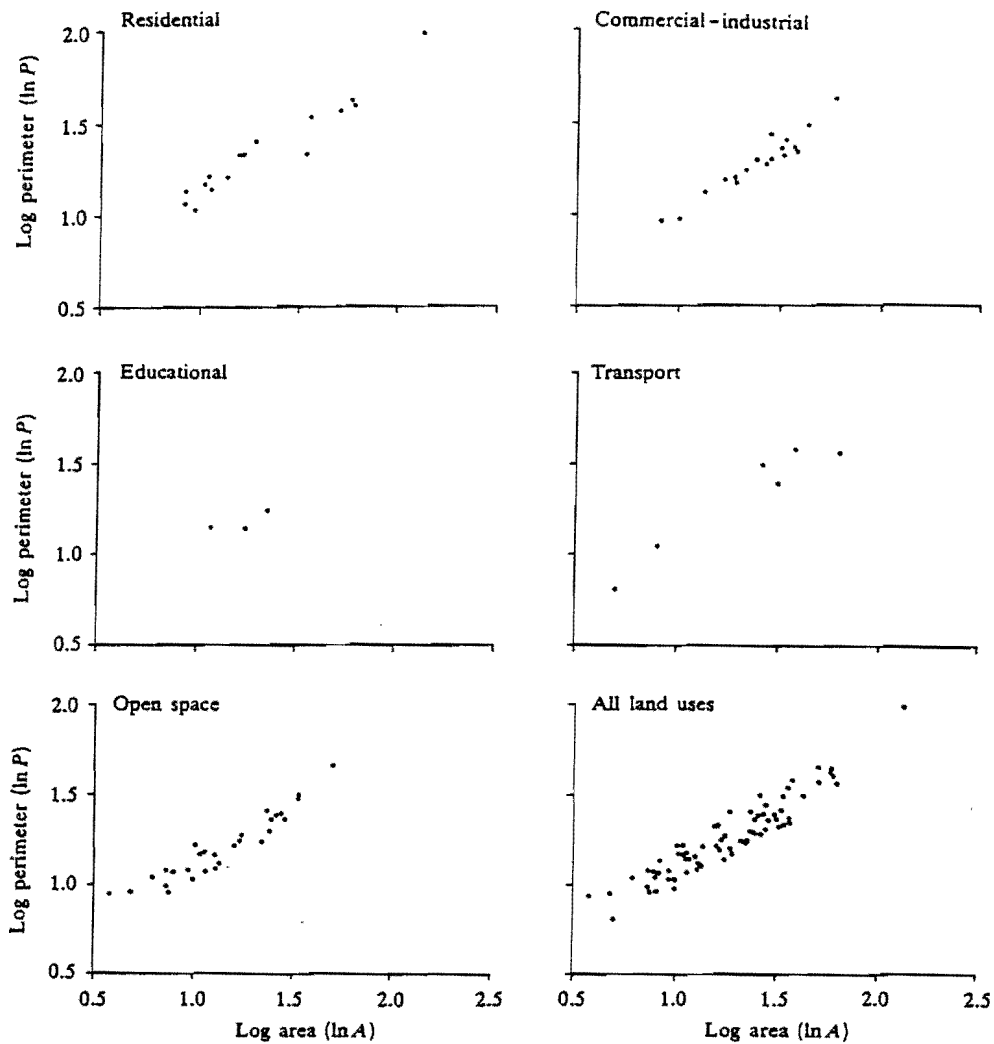


Figure 3. Scatter plots of area-perimeter relations.

Table 1 (continued).

Land use	Mean number of points per parcel	Average chord length Δx	Perimeter $P = \Delta x N$	Feret's diameter
Residential	186.8	0.7848	2344.9	119.5
Commercial-industrial	57.2	0.8375	861.8	42.4
Educational	36.3	0.7266	78.5	11.5
Transport	85.0	0.8206	417.7	52.8
Open space	49.0	0.7760	1106.2	52.9
All land uses	84.2	0.7949	4816.3	119.5

Table 2. Parameters associated with the area-perimeter relations.

Land use	Conventional model ^a		Modified model ^b		
	D	$100 \times R^2$	c	d	$100 \times R^2$
Residential	1.3310	92.4	0.4996	0.2289	92.5
Commercial-industrial	1.4779	92.3	0.3068	0.3608	92.6
Educational	0.5694	11.1	-15.4265	5.4611	not computed
Transport	1.4471	91.3	3.9956	-0.8450	95.0
Open space	1.2435	89.2	-0.7104	0.6932	92.5
All land uses	1.2961	88.0	0.3398	0.3006	89.2

^a See equation (18) in text.
^b See equation (19) in text.

Estimation using aggregated perimeter-scale relations

Before we introduce the analysis based on perimeter-scale relations, it is worth discussing the degree of irregularity associated with different land-use patterns as we perceive them in a priori terms. In examining the five land uses, we might argue that open space is more likely to be defined according to the boundaries imposed by natural terrain, in contrast to more artificially determined land uses such as the commercial-industrial and transport uses. Residential land use is likely to have a degree of irregularity in its form somewhere between these extremes, as might educational use. With respect to the area-perimeter relations, this a priori ranking of open space, residential, educational, commercial-industrial, transport is not borne out at all by the fractal dimensions. Indeed, table 2 implies somewhat the reverse, but the R^2 s are lower than anticipated and it is possible that area-perimeter relations do not capture scale effects to the same precision as methods based on perimeter-scale relations.

However, to be consistent with the area-perimeter analysis, it is necessary to devise a way of determining single fractal dimensions for each set of land parcels according to land-use types. In a later section, we will look at the variation in fractal dimension across land parcels and types, but here we will begin by defining a global (or total) perimeter for each land-use set. Were we simply to calculate a single total perimeter for each land use based on all its parcels, and regress these against scale, this would be similar to our previous analysis as scale would be a proxy for area. What we have done in fact is to calculate a total perimeter for each land use by stringing together the individual land-parcel perimeters in the arbitrary order in which the parcels and their coordinate points have been digitised. We have also derived a total of total perimeters in the same way which contains all the points relevant to each land parcel over all land uses.

In figure 4, we show these total perimeters for each of the five land uses. These are *not* drawn to the common scales of the parcels contained in figures 1 and 2, but are scaled up or down to be roughly comparable in area when displayed on a graphics terminal. It should be quite straightforward to identify the land parcels from their classification in figure 2. The total perimeters are in fact derived by centring the first digitised point of each land parcel on a common point and producing a string of coordinates in the order in which each land use was digitised. The educational and transport land uses with the fewest land parcels show this most clearly in figure 4. We have not included the total of total perimeters because it is not possible to produce a clear and clean plot as a result of the continual overlapping of boundaries; we will, however, use this total in the subsequent analysis.

From these base-level perimeters, aggregations across the given range of scales yielding approximate perimeters provide the data for estimating the parameters of the perimeter-scale relation. Two issues are important. First, the order and orientation of the land parcels forming the total perimeter could be crucial, and second the aggregations should not be so great as to pick up the aggregate shape of these composite perimeters which is clearly quite arbitrary. Order and orientation have been varied and this makes little difference to the subsequent results, but the

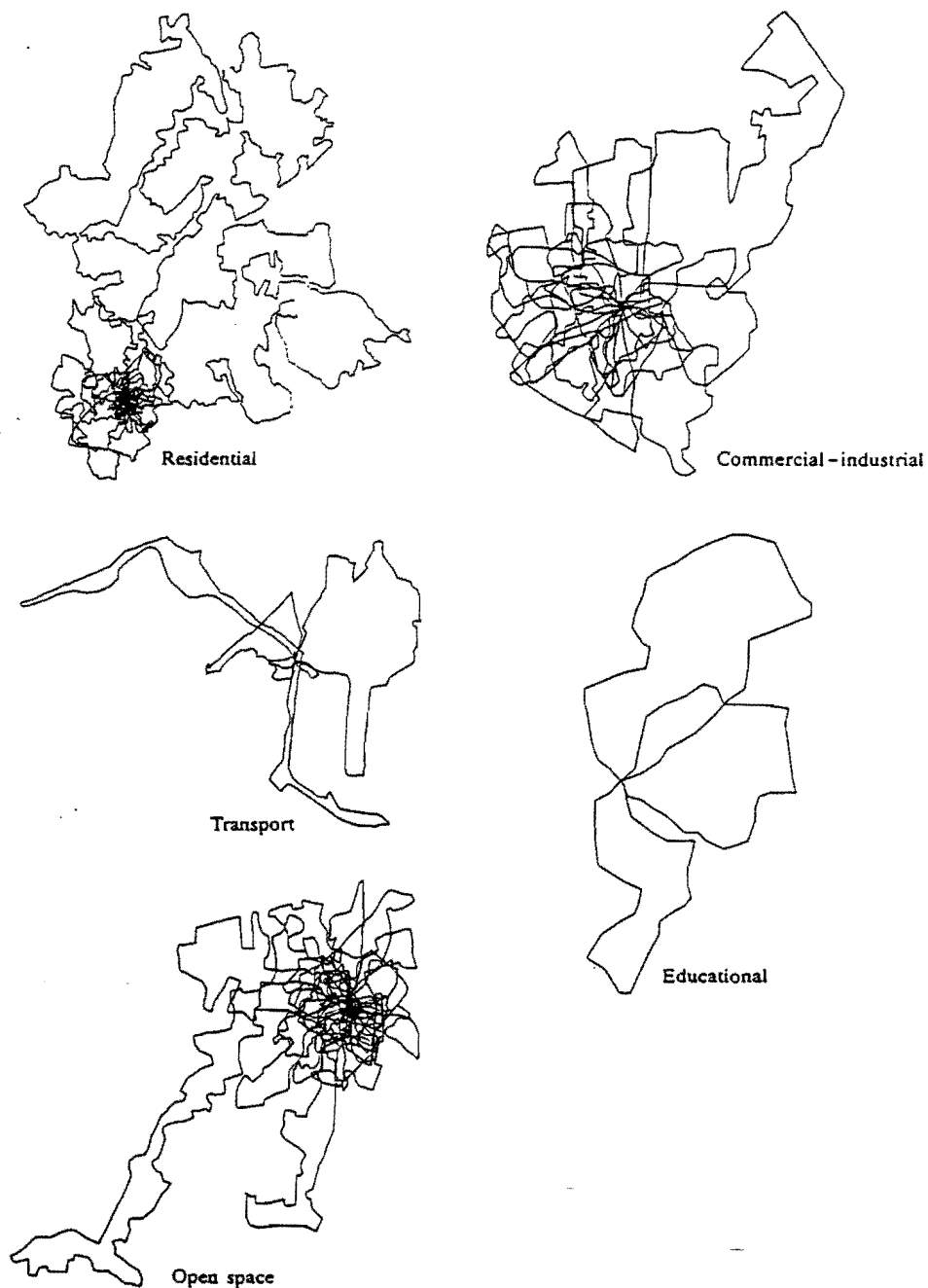


Figure 4. Aggregate perimeters for the five land uses.

aggregate shape problem does affect the estimated dimensions. In fact, this leads to a reestimation of the perimeter-scale relations with a reduced set of aggregations which will be reported in the next section.

The number and scale of the aggregations for each of these perimeters, which provide the set of observations for the log-log regressions, are fixed so that each observation is of equal weight in the estimation. The limits of aggregation for the structured walk, hybrid walk, and cell count methods are first calculated as follows. The maximum spanning distance or Feret diameter, F , is computed from

$$F = \max_{ij} \{d_{ij}\}, \quad \text{where} \quad \left. \begin{array}{l} \\ d_{ij} = [(x_i - x_j)^2 + (y_i - y_j)^2]^{1/2}; \end{array} \right\} \quad (20)$$

d_{ij} is the distance between two distinct points referred to as i and j in the base-level N -coordinate data set which defines the total perimeter from the coordinate pairs x_i, y_i ($i = 1, \dots, N$). The average chord length, \bar{d} , in this data set is given as

$$\bar{d} = \sum_i \frac{d_{i,i+1}}{N-1}, \quad (21)$$

where there are $N-1$ chords making up the base-level perimeter.

The sequence of aggregations where \bar{d} represents the first chord size and F represents the last, and where m is the number of aggregations, is given by

$$F = \alpha^{m-1} \bar{d}. \quad (22)$$

In fact, the starting point is set as the minimum, not average, chord size, and this can be represented as a fraction, μ , of \bar{d} . Therefore, equation (22) becomes

$$\mu F = \alpha^{m-1} \mu \bar{d}. \quad (23)$$

The weight α scales one chord size to the next in the sequence of aggregations and this is computed from equations (22) or (23) as

$$\alpha = \exp\left(\frac{\ln F - \ln \bar{d}}{m-1}\right). \quad (24)$$

This method of aggregating perimeters can only be applied to the structured walk, hybrid walk, and cell count methods of approximation, for the equipaced polygon method does not involve distances between points, only the order of points in the base-level data set.

A similar method of weighting is used, however, involving numbers of base-level chords, not length based on distances. As the number of base-level chords used to form a new chord increases, the actual length of the new chord increases and this is akin to aggregation to larger distance scales. Then, if the number of original points needed to approximate the coarsest acceptable perimeter is N_{\max} and the minimum number N_{\min} , the sequence of chord sizes in the sequence of aggregations is given as

$$N_{\max} = \alpha^{m-1} N_{\min}, \quad (25)$$

from which α is determined in the same way as previously; that is, as

$$\alpha = \exp\left(\frac{\ln N_{\max} - \ln N_{\min}}{m-1}\right). \quad (26)$$

In fact, N_{\min} is always 2, and N_{\max} is set as $N/6$, thus implying that the number of chords defining the most aggregate perimeter is 6; this would make the top level of aggregation reasonably consistent with the maximum spanning distance F .

The algorithm used to aggregate the original chords on each iteration into new perimeters uses α in equation (26) only as a guide. Clearly the number of chords must be integral, not real, thus equation (25) involves truncation or addition to create integer numbers. The number of aggregated chords on each iteration $n+1$ is given as $N_{n+1} = \text{int}(\alpha N_n)$. However, if N_{n+1} is equal to N_n , then N_{n+1} is increased by one chord length, that is $N_{n+1} = N_n + 1$. In the application of these algorithms, we have set m as 100 in each case. In fact, for the equipaced polygon method, although this also applies, the actual number of aggregations made is always less than 100 because of the discrete conditional nature of the aggregation.

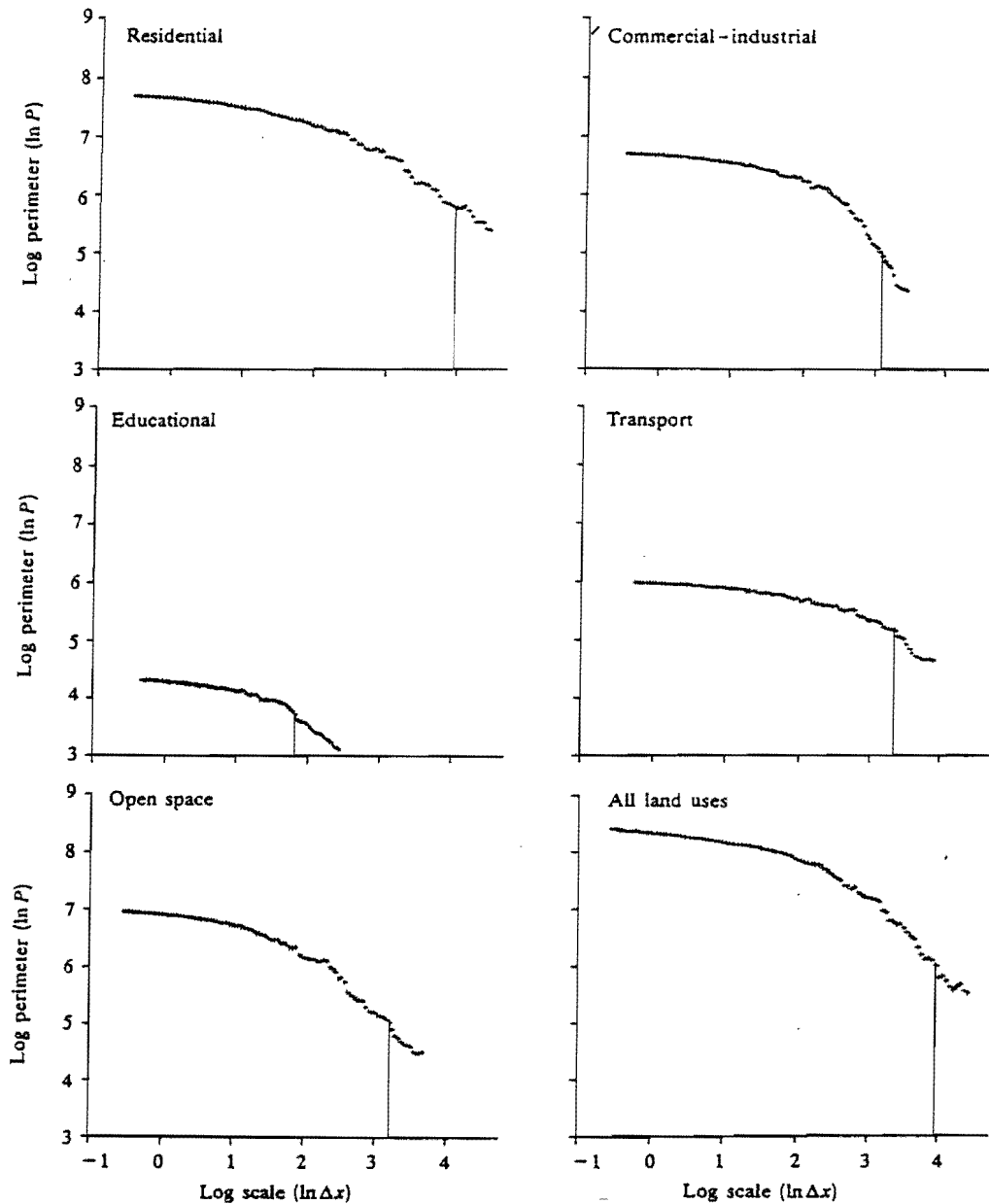


Figure 5. Richardson plots of perimeter-scale with the structured walk method.

The observations produced by applying each of these four methods to the five total perimeters and the total of totals are shown as Richardson plots in figures 5-8. Before the associated regressions are discussed there are several points to note. First, there are quite clear upper scale effects caused by aggregation to too high a level. These are seen as departures from the trend of each graph and as obvious twists and turns in the tails of some of the plots. Second, these plots show strong evidence of nonlinearity suggesting, as in previous work (Batty and Longley, 1987b; Orford and Whalley, 1983), that the modified model, where fractal dimension varies with scale, is more applicable than the conventional model. Third, the equipaced polygon method gives cause for concern in that the algorithm attempting equal

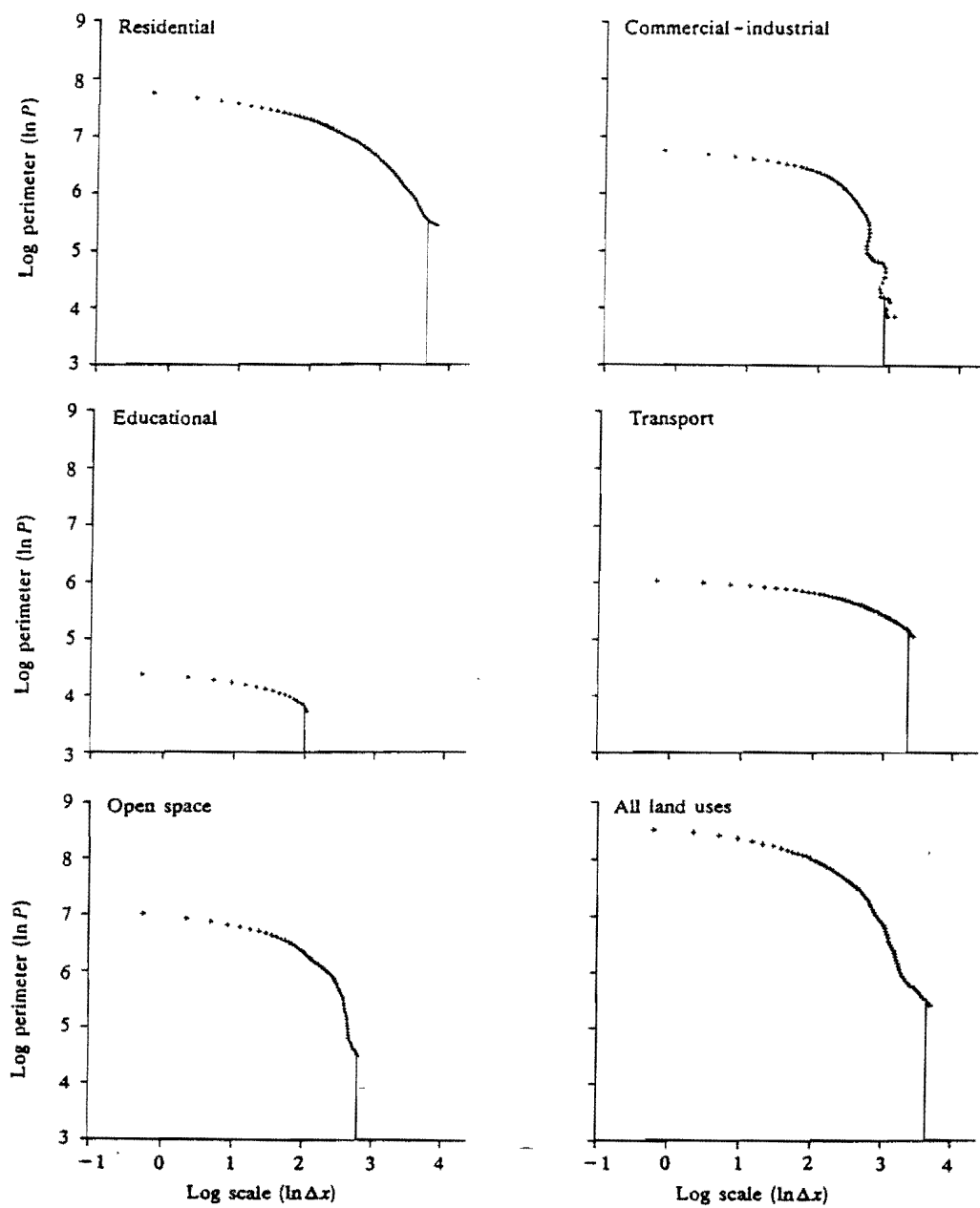


Figure 6. Richardson plots of perimeter-scale with the equipaced polygon method.

weighting does not perform well in establishing equal spacing of observations or in meeting the fixed number ($m = 100$) of aggregations; and there are clear twists in the tails of the associated plots at the higher levels of aggregation. Last, the aggregation, in the case of educational land use, over 100 levels is problematic in that there are only 109 digitised points in the total perimeter set as shown in table 1.

We will present the fractal dimensions derived from the conventional and modified models for all the plots shown in figures 5-8, notwithstanding the fact that the equipaced polygon method and educational land use are, in the sense just described, likely to yield unreliable results. In table 3, we show the fractal dimension D computed from the slope of the regression line, $g(D) = 1 - D$, as in equation (9)

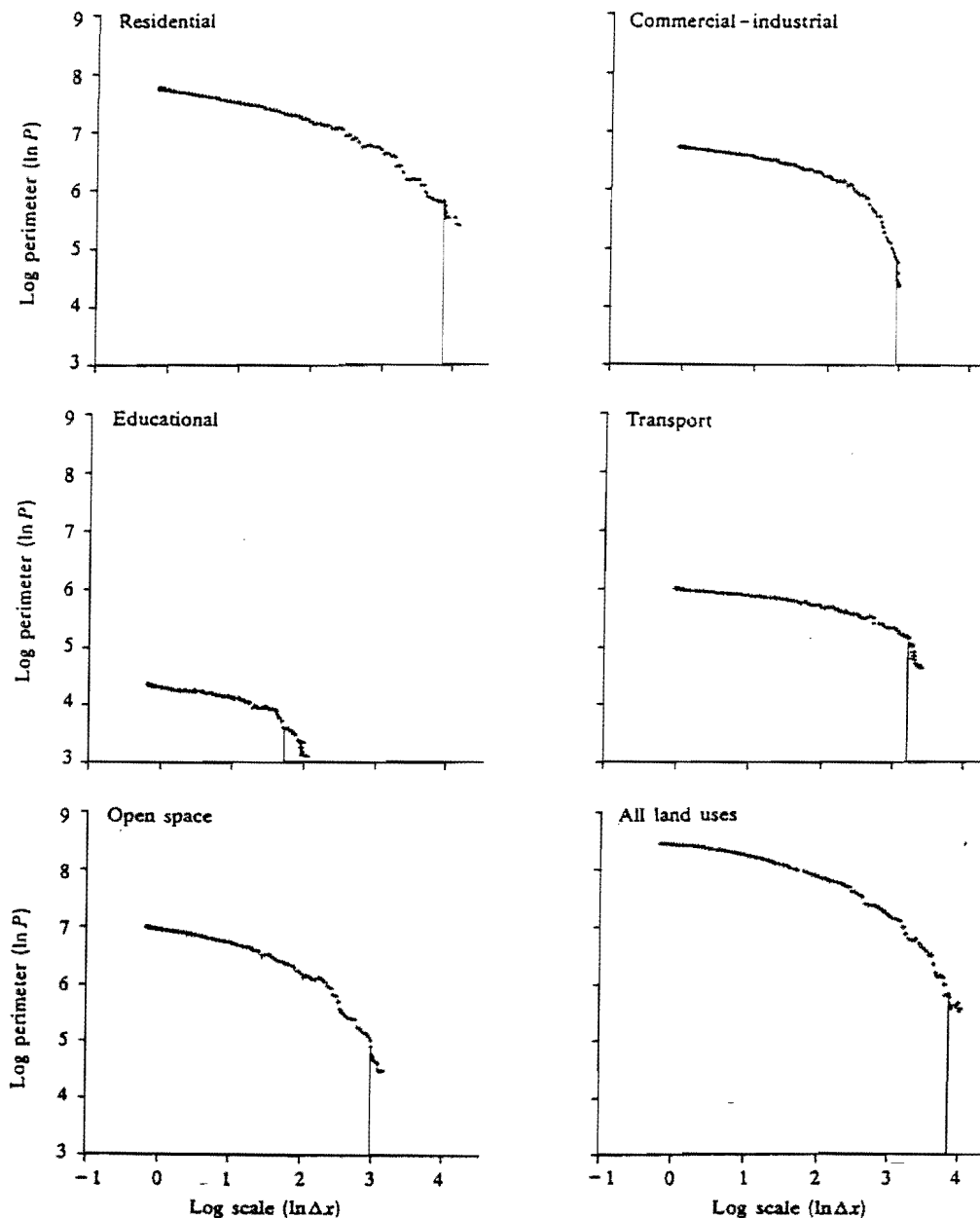


Figure 7. Richardson plots of perimeter-scale with the hybrid walk method.

applied to equation (15) which involves the conventional model; and we also show the performance of the model in terms of $100 \times R^2$ statistics. In table 4, we show the same for the modified model as given in equation (17). In this table, we first give the fractal dimension D derived from the coefficient a as $1 - a$, and then we give the dispersion coefficient, b , noting of course that as $b \rightarrow 0$, $D \rightarrow 1 - a$.

It is immediately clear from tables 3 and 4 that the modified model in which dimension is a function of scale gives by far the best performance over all methods and land uses. Yet the equipaced polygon and hybrid walk methods produce strange results for the modified model, in that fractal dimensions are less than 1 in four cases. In the case of the conventional model, these methods also appear to give D values higher than anticipated. With respect to the ranking of D values

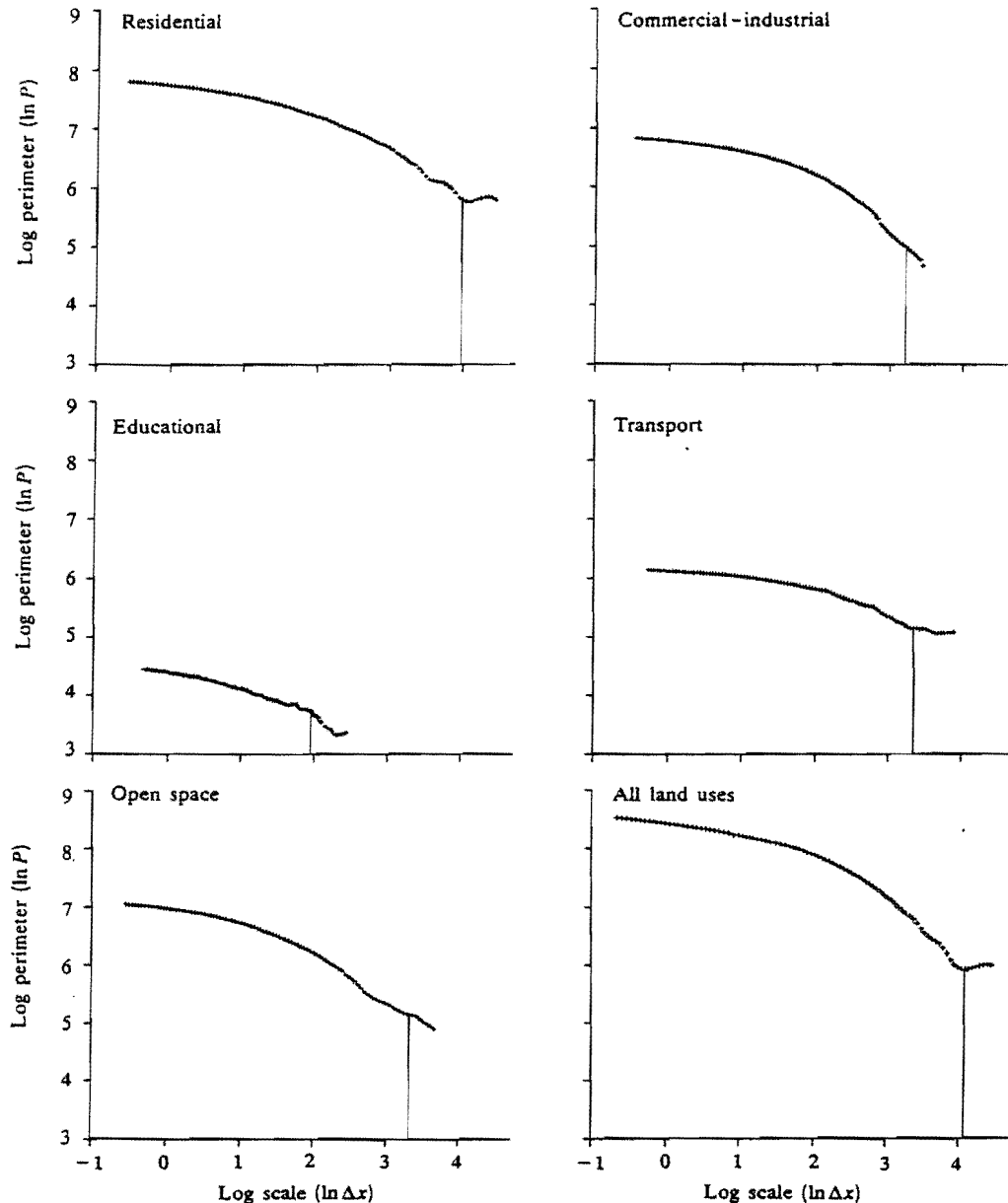


Figure 8. Richardson plots of perimeter-scale with the cell count method.

from table 3, there is, however, a fairly consistent order over all methods in which open space, all land uses, and commercial-industrial have higher fractal dimensions than residential, which in turn is higher than educational and transport.

A more disordered set of ranks is associated with the modified model, although there are some similarities with the conventional model results, and in any case, the dispersion coefficients pick up the nonlinearity in the relations and hence influence the value of D . In this respect, the dispersion coefficients are quite low for most land uses. To summarise, then, if the equipaced polygon and hybrid methods which seem to pick up inappropriate larger scale effects, are ignored, the structured walk and cell count methods produce a ranking of fractal dimensions across all land uses (with the exception of educational) according to our a priori expectations. At this stage, it is even possible to say that variations in dimension and coefficients between land uses are clearly wider than between methods, and this implies that the choice of method is less significant than the division into standard types of land use.

Table 3. Fractal dimensions based on the conventional model.

Method ^{a,b}	Residential	Commercial- industrial	Educational	Transport	Open space	All land uses
Structured walk	1.4505 (90.3)	1.5080 (77.3)	1.3964 (84.2)	1.2896 (83.6)	1.5927 (88.0)	1.5702 (86.7)
Equipaced polygon	1.6941 (85.3)	2.0660 (61.9)	1.2738 (82.7)	1.3004 (81.1)	1.9566 (68.7)	2.0208 (79.5)
Hybrid walk	1.4957 (90.4)	1.5661 (75.7)	1.4424 (79.9)	1.3137 (80.3)	1.6656 (86.0)	1.6191 (86.2)
Cell count	1.4475 (93.9)	1.4988 (87.2)	1.4016 (94.6)	1.2936 (92.0)	1.5429 (93.7)	1.5713 (90.9)

^a The structured walk, hybrid walk, and cell count methods are based on 100 aggregations for each land use (that is, $m = 100$). The equipaced polygon method has $m = 72, 68, 17, 53, 65$, and 75 for the five land uses and all land-use applications. These m values also pertain to the modified model results in table 4.

^b The entries in the table are the fractal dimension, $D = 1 - g(D)$, with the $100 \times R^2$ statistic given in parentheses.

Table 4. Fractal dimensions based on the modified model.

Method ^{a,b}	Residential	Commercial- industrial	Educational	Transport	Open space	All land uses
Structured walk	1.2721 -0.0036 (98.1)	1.0757 -0.2121 (99.5)	1.0576 -0.0408 (99.1)	1.0957 -0.0058 (99.2)	1.2917 -0.0122 (98.0)	1.2907 -0.0056 (98.1)
Equipaced polygon	1.1873 -0.0107 (99.7)	0.5588 -0.0608 (94.1)	1.0058 -0.0359 (98.8)	1.0453 -0.0075 (99.9)	0.7161 -0.0637 (95.6)	1.1758 -0.0199 (97.4)
Hybrid walk	1.2499 -0.0062 (99.4)	0.9563 -0.0365 (97.7)	0.9254 -0.0818 (97.8)	1.0401 -0.0108 (97.4)	1.1575 -0.0272 (99.6)	1.2253 -0.0098 (99.6)
Cell count	1.3327 -0.0023 (97.2)	1.2039 -0.0145 (99.3)	1.2235 -0.0215 (99.1)	1.1903 -0.0031 (96.8)	1.3747 -0.0068 (97.6)	1.3744 -0.0040 (96.7)

^a See footnote a, table 3.

^b The entries in the table are the fractal dimension, $D = 1 - a$ and the dispersion coefficient, b , with the $100 \times R^2$ statistic given in parentheses.

However, the really important point at issue here is the presence of unwanted and arbitrary scale effects in the data. It is quite clear from figures 5-8 that we must remove the highest aggregations from all these plots. In doing so, we also immediately remove some of the nonlinearity from the data, thus hopefully improving the conventional model estimates as well as resolving some of the anomalous dimensions evident in tables 3 and 4.

Reestimation of the perimeter-scale relations

The range of aggregations with respect to the structured walk, cell count, and hybrid walk methods as given in equations (23) and (24) begins with the first and last chord lengths set as low as 70% of the average distance, \bar{a} , and Feret diameter, F , for residential land use, to as high as 99% of \bar{a} and F for the educational land use. Shelby et al (1982) recommend that the starting points should be no lower than $\frac{1}{2}\bar{a}$ and Kaye (1978) recommends the end point be no higher than $\frac{1}{2}F$. The lower limits ($\mu\bar{a}$) we have used do not pose any problem, but the upper limits (μF) yield approximations to the total perimeter with as few as two chords and only as many as five chords. An approximation to the boundary of any irregular object can never be made in less than six chords and in the case where we have up to thirty land parcels forming an aggregated perimeter, it could be argued that we should never go below 180 chords. Below this level we unwittingly include scale effects which pick up the arbitrariness of the 'constructed' perimeters; these are also sensitive to order and orientation of the land-parcel strings. In terms of this argument, it would appear that we should take an upper limit no greater than 20% of Feret's diameter, that is $\mu = 0.2$.

From an examination of figures 5-8, it is quite straightforward to determine cutoff limits at the upper tails of each plot which would remove those observations clearly sensitive to these unwarranted scale effects. We have defined these cutoff limits in these figures, showing the number of observations each set has been reduced to. This varies for the structured walk methods from 9% to 22% of the original set to as little as between 5% and 10% in the case of the equipaced polygon methods. From figures 5-8, it is clear that we could impose even harsher constraints on the observations used, but, although this would probably improve the results still further, relevant scale effects would probably be removed too.

Tables 5 and 6 show the reestimations of the two models using the four methods applied to each land use and the total of all land uses. There are marginal increases in the performance of the conventional model as comparisons between

Table 5. Reestimation of the fractal dimensions for the conventional model.

Method ^{a,b}	Residential	Commercial- industrial	Educational	Transport	Open space	All land uses
Structured walk	1.4031 (89.2)	1.3888 (78.6)	1.2291 (91.0)	1.2099 (89.7)	1.4992 (86.9)	1.4861 (86.4)
Equipaced polygon	1.6629 (85.0)	1.7472 (62.4)	1.2437 (86.0)	1.2732 (82.3)	1.9163 (68.9)	1.9933 (78.7)
Hybrid walk	1.4578 (91.1)	1.4769 (79.3)	1.2907 (85.3)	1.2393 (89.5)	1.5735 (87.7)	1.5596 (86.9)
Cell count	1.4225 (92.5)	1.4516 (87.0)	1.3289 (98.0)	1.2627 (89.2)	1.5158 (92.4)	1.5408 (89.1)

^a The numbers of observations used for each regression are indicated in figures 5-8.

^b The entries in the table are the fractal dimension, $D = 1 - g(D)$, with the $100 \times R^2$ statistic given in parentheses.

tables 3 and 5 indicate. There is increased consistency between the methods with respect to the dimensions estimated, with the exception of the equipaced polygon method. This is the most volatile of all the methods, with the structured walk being the most consistent in terms of the original estimation and the reestimation. With respect to the ranking of land uses by dimension, an even clearer pattern emerges. Those with the higher fractal dimensions are open space and all land uses, then commercial-industrial and residential, with much lower dimensions for educational and transport uses. This bears out the a priori analysis even more strongly, but it must be noted that the performance of the conventional model is only just adequate.

The modified model results shown in table 6 are even better than those of table 4. The ranking pattern is more variable than that of the conventional model with the commercial-industrial, educational, and open space land uses having the highest degree of nonlinearity as measured by the dispersion coefficient. The equipaced polygon method somewhat ironically perhaps, has by no means the worst performance, but it still generates coefficients out of line with the other methods. As with the conventional model, the structured walk provides the most consistent results over each land use, and together with the cell count method gives the best performance.

It is now worth summarising all these results with respect to the fractal dimensions produced. In figure 9, an attempt is made to capture the variations in dimension obtained across all methods and land uses in a single diagram. Each of the diagrams shows this variation with respect to the area-perimeter, conventional perimeter-scale, and modified perimeter-scale methods, the last two being shown with respect to their original estimation and reestimation. It is quite clear from these plots that the equipaced polygon method is the most problematic and should be excluded. Yet the structure of these results does show that there are greater differences between land uses than between methods, and this bears out the original hypothesis that such differences can be detected and possibly explained with respect to the processes governing the formation and evolution of different land-use activities. We will say more about this in our conclusion, but before we explore the variations between land parcels, we have averaged the dimensions produced in the last three sections, and these are shown, together with those of the subsequent section, in table 7.

Table 6. Reestimation of the fractal dimensions for the modified model.

Method ^{a,b}	Residential	Commercial- industrial	Educational	Transport	Open space	All land uses
Structured walk	1.2128 -0.0059 (99.0)	1.0497 -0.0233 (99.6)	1.0696 -0.0346 (98.6)	1.0938 -0.0058 (99.3)	1.2028 -0.0187 (98.6)	1.2195 -0.0082 (99.1)
Equipaced polygon	1.1618 -0.0115 (99.9)	0.7001 -0.0515 (92.1)	1.0302 -0.0311 (99.6)	1.0479 -0.0074 (99.9)	0.0739 -0.0622 (95.2)	1.1175 -0.0219 (98.0)
Hybrid walk	1.2373 -0.0067 (99.4)	1.0167 -0.0307 (98.8)	1.0236 -0.0574 (96.1)	1.0929 -0.0072 (99.4)	1.1765 -0.0259 (99.5)	1.2158 -0.0101 (99.7)
Cell count	1.2609 -0.0050 (99.2)	1.1657 -0.0175 (99.7)	1.2494 -0.0151 (99.1)	1.1105 -0.0076 (99.6)	1.3035 -0.0117 (98.4)	1.2846 -0.0072 (99.1)

^a The numbers of observations used for each regression are indicated in figures 5-8.

^b The entries in the table are the fractal dimension, $D = 1 - a$ and the dispersion coefficient, b , with the $100 \times R^2$ statistic given in parentheses.

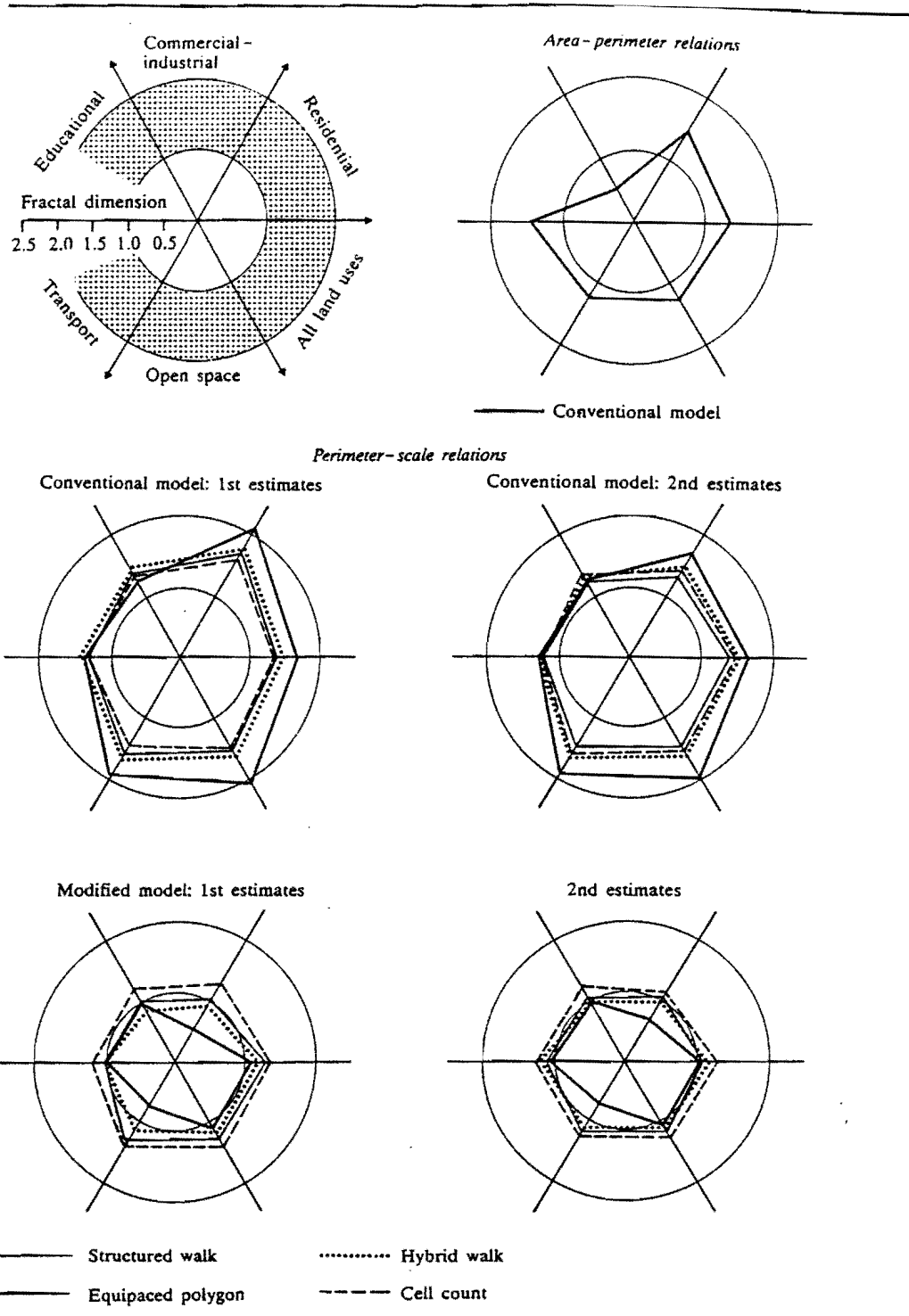


Figure 9. Variations in fractal dimensions with respect to models, methods, and land uses.

It is clear that the area-perimeter method produces quite different results from the perimeter-scale methods, but that the patterns produced by the perimeter-scale methods are more robust and consistent with our a priori theorising. For the conventional model, the fractal dimensions vary from $D \sim 1.55$ for open space and all land uses to $D \sim 1.45$ for residential and commercial-industrial to $D \sim 1.30$ for educational and transport. With respect to the modified model $D \sim 1.25$ (in its limit) for open space, all land use, and residential, whereas for the other three land uses, $1.00 \leq D \leq 1.10$. This implies that these last three land uses present greater nonlinearity; that is, their fractal dimensions vary more strongly with scale. These results mask the wide variation in dimension between land-use parcels within any land-use type, and do not in any way address the equality of fractal dimension over common boundaries between different land uses. We will address some of these questions in the next section.

Table 7. Fractal dimensions 'averaged' over methods of aggregation.

Method/model	Residential	Commercial- industrial	Educational	Transport	Open space	All land uses
<i>Area-perimeter method</i>						
Conventional model	1.33	1.47	0.56	1.45	1.24	1.29
<i>Perimeter-scale method</i>						
Conventional model						
1st estimates	1.46	1.52	1.41	1.29	1.59	1.58
2nd estimates	1.42	1.43	1.28	1.23	1.51	1.52
Modified model						
1st estimates	1.28	1.07	1.06	1.10	1.27	1.29
2nd estimates	1.23	1.07	1.10	1.10	1.22	1.23
<i>Average land parcels</i>						
Conventional model	1.15	1.10	1.09	1.11	1.13	1.13
Modified model	1.08	1.05	1.05	1.06	1.08	1.07

Fractal dimensions of individual land parcels

Figure 2 shows that there are seventy-two distinct land-use parcels, although in the previous analysis the inner boundaries of some residential land parcels, where such boundaries existed, were added to the aggregate perimeters. There are eight such inner boundaries, all relating to residential land use as shown in figure 2, and in the subsequent analysis they are treated as separate land parcels, thus augmenting the number of parcels treated to eighty. First, all four aggregation methods—the structured and hybrid walks, the equipaced polygon, and the cell count methods—were applied to each of the eighty parcels, with the number of aggregations structured in geometric form as implied by equations (21)–(25) but with α fixed and m varied accordingly.

In the case of the equipaced polygon method, the aggregation of sixteen perimeters out of the eighty possible yielded too few observations for any subsequent regression. The other methods produced Richardson plots that were generally more linear than those shown in figures 5–8 and therefore it was decided to fit the conventional model to all sets of observations generated. The R^2 -values ranged from 83.3% to 99.9% in the case of applying the equipaced polygon method, but it was the structured walk that produced the most consistent plots in contrast to the hybrid and cell count methods which were more volatile across the land parcels. Some methods produced dimensions for individual land parcels outside the range $1 < D < 2$. It was therefore decided to pursue more detailed analysis and model fitting using a narrower range of observations taken from the structured walk

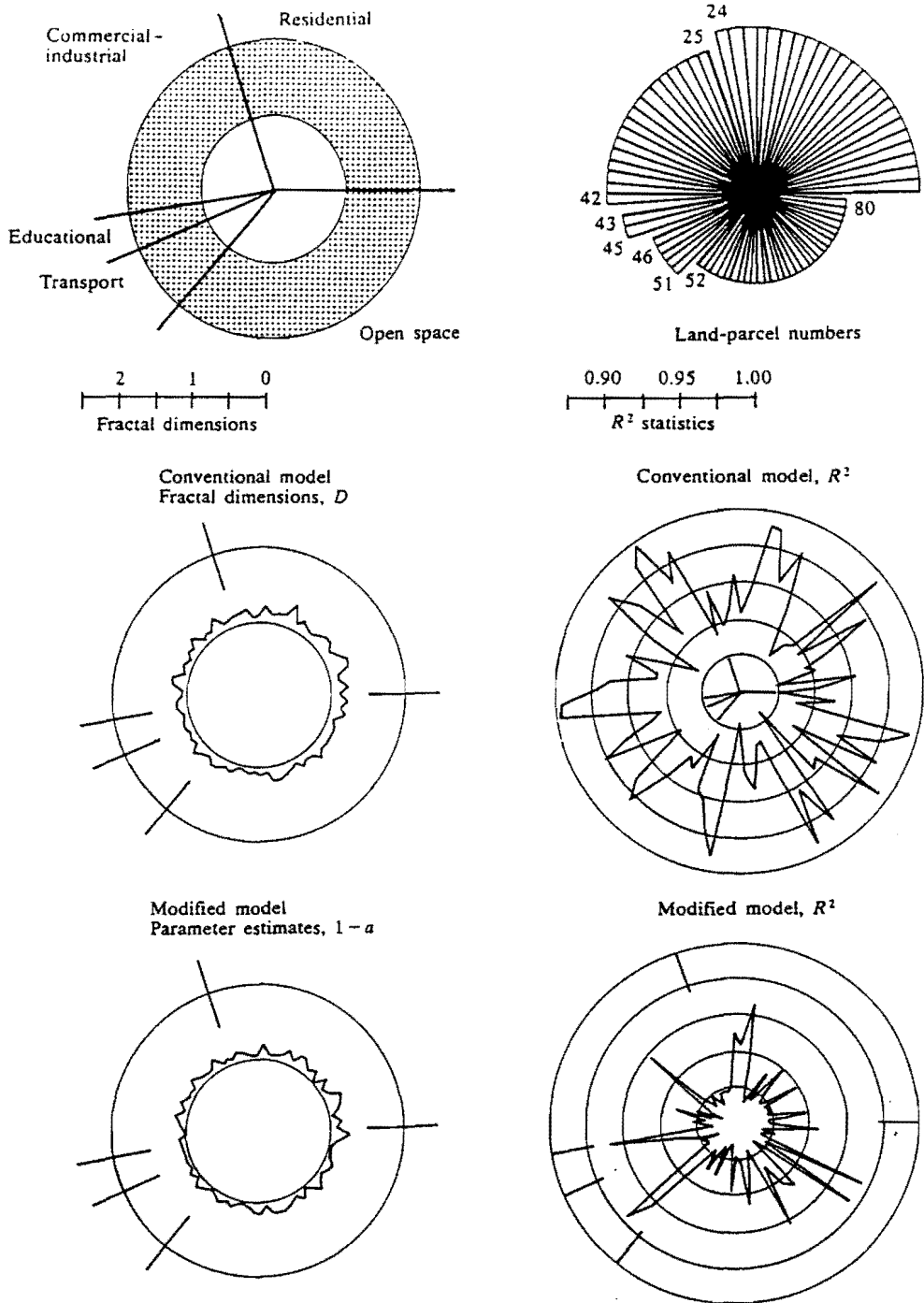


Figure 10. Fractal dimensions of individual land parcels.

method only. In fact, the emphasis in this section is on the variation between land parcels, not on the variation between methods, hence the choice of the most robust method to generate the perimeter-scale observations.

The application both of the conventional and of modified models is shown in figure 10 with respect to their fractal dimensions and associated R^2 -statistics. The results for each land parcel are shown in the arbitrary order of figure 2 according to the way the parcels were digitised but ordered within land-use types as given previously. All fractal dimensions for the conventional model are in the postulated range from $1 < D < 2$. For the largest land parcels, the dimensions appear higher than for the rest but a regression of the number of digitised points of all parcels on their conventional model dimensions yields an R^2 -value of only 15.6%. With respect to the five sets of land uses, these R^2 -values were more variable, rising to 68.6% in the case of commercial-industrial. But in general, there does not appear to be a strong bias to higher dimensions for those land-use parcels with the highest number of perimeter coordinates. Figure 10 also shows that the parameters of the modified nonlinear model are consistent with the range of $1 < D < 2$, and the level of dispersion reflecting the nonlinearity of each parcel over scale, is fairly modest in every case.

One way of summarising these parameters and statistics is by computing means and standard deviations. Table 8 presents these results for both models. The parameters and dimensions in this table are in their original form as predicted from the application of equations (15) and (17), that is, the coefficient of the conventional model is a , $a = g(D) = 1 - D$, and the coefficients for the modified model are a and b , where $a \rightarrow (1 - D)$ as $b \rightarrow 0$ (b is the dispersion parameter). Table 8 presents the variation in size of the land parcels for each land use and over the whole set in terms of their mean number of coordinates. The distribution of these coordinates with respect to the number of land parcels is skewed, with a much greater proportion of parcels below their mean size. In the case of the residential parcels, this distribution is highly skewed, largely because of the existence of the one large parcel which provides the skeletal structure of the town.

The variation in parameters and performance of the models, however, is much less than the variation in the features of the land parcels themselves. Figure 10 makes this apparent, and these results are averaged for each land use over all parcels in table 8. With respect to the conventional model, the R^2 -values only range from 93.4% in the case of residential parcels down to 91.9% for transport and the range with each land use over the land parcels is also quite narrow. The fractal dimensions D also show a pattern over the land uses which is consistent with the aggregated perimeter-scale results but is considerably clearer. The ranking of land uses from largest to smallest D is ordered from residential ($D = 1.15$), open space (1.13), transport (1.11), commercial-industrial (1.10), and educational (1.09) with an average over all land uses of 1.13. These values are considerably smaller than those shown previously, yet they are more in line with previous work (Batty and Longley, 1987a; 1987b). In fact, the largest residential parcel (see figure 2) is just one of five parcels which has a dimension greater than 1.20. From these results it is quite clear that the much higher dimensions produced by the aggregated perimeter-scale relations are caused by the method of aggregating individual perimeters into strings of coordinates. It would appear that the aggregation picks up arbitrary scale effects which are central to the method itself and not the order or orientation of the individual parcels in the process of forming these composite perimeters.

The modified model results also shown in table 8 have a wider range of variation around their mean estimates than those of the conventional model. In terms of the

Table 8. 'Average' dimensions and statistics for the individual land parcels.

	Zones	Total no. of coordinates	Mean no. of coordinates	σ_c	$a = 1 - D_1$	σ_{D_1}	$100 \times R^2$
Residential	24	2989	124.5	317.2	-0.152	0.063	93.4
Commercial-industrial	18	1030	57.2	33.3	-0.105	0.061	92.0
Educational	3	109	36.3	6.65	-0.091	0.035	92.1
Transport	6	510	85.0	65.8	-0.113	0.040	92.0
Open space	29	1421	49.0	38.9	-0.132	0.046	92.8
All land parcels	80	6059	75.7	177.4	-0.129	0.057	92.7

Note: The standard deviations are defined as: σ_c of the coordinates, σ_{D_1} of the slope parameter a in the conventional model, σ_{D_1} of the parameter a in the modified model, σ_b of the parameter b in the modified model, and σ_{R^2} of the R^2 fits of the appropriate model to the land-parcel data.

ranking of the parameter a , the residential, open space and all land-use parcels have a dimension higher than those of transport, commercial-industrial, and educational, in that order, although these values are over a narrower range. The values of the dispersion factors show this order and the R^2 -estimates, although slightly better than those of the conventional model, are not as high as those produced by the aggregate perimeter-scale relations. Nevertheless, the nonlinear model is an improvement over the linear and, in general, these results for the individual parcels are better than originally anticipated.

Conclusions

The analysis presented here is generally inconclusive. At most, it would appear that residential and open space land uses have a greater degree of irregularity than commercial-industrial, educational, and transport. There is a logic here which we spelt out before we began the analysis in that, for land uses which are larger in scale, there is likely to be less effort put into the geometric control of land under development. Yet there remains considerable uncertainty over the processes in operation. We have, however, shown that, in general, scale effects vary with scale itself, and this is likely to be the result of multiple processes changing their relative importance through the range of scales. This argument was spelt out by Batty and Longley (1987b) and is further confirmed here.

We have added to table 7 the results of the last section where the whole range of models and methods applied throughout this paper are displayed in suitably 'averaged' form. This shows up the arbitrariness of the analysis, with open space varying from $D \sim 1.59$ to $D \sim 1.13$ and residential land use from $D \sim 1.46$ to $D \sim 1.15$ for the linear conventional model. In previous work, the methods themselves have been subject to considerable variation, but here despite some mild association of dimension values with land uses, the main variation concerns the way area, perimeter, and scale are defined and the type of approach or method taken.

Questions of scale are never very clear in much fractal analysis, despite the fact that fractals are defined by scale-invariance. In the area-perimeter method it is assumed that objects of varying sizes show the effects of varying scale itself (Woronow, 1981). In short, a small residential development will not pick up the aggregate scale effects which can be detected by a large-scale development; so

Table 8 (continued).

σ_{R^1}	$a = 1 - D_2$	σ_{D_2}	b	σ_b	$100 \times R^2$	σ_{R^1}
3.3	-0.079	0.063	-0.029	0.022	97.2	1.8
3.1	-0.050	0.042	-0.018	0.011	97.9	1.6
4.3	-0.047	0.005	-0.022	0.018	95.2	3.1
2.2	-0.065	0.028	-0.006	0.001	96.0	3.9
3.6	-0.077	0.048	-0.030	0.025	96.6	2.3
3.3	-0.071	0.051	-0.024	0.021	96.9	2.3

runs the logic. However, this will depend on the base level of resolution in the first place and there is seldom much discussion of this in the literature. The method of aggregating perimeters used in the composite perimeter-scale analyses of land uses, is also suspect because of arbitrary scale effects which can be produced, despite careful control over the process of aggregation. Last the individual land-parcel analysis using conventional perimeter-scale, not aggregated relations, suffers from its very inability to aggregate parcels, other than by arbitrary statistics such as simple averages.

What is clearly required in future work is a close examination of these approaches in terms of scale effects. We have paid great attention to problems of defining scale limits and ranges here, but on reflection, our analysis should have reduced the range of scales much further. New methods are required which are more robust than those used here, and we should now accept that in the perimeter-scale analysis, the hybrid walk and equipaced polygon methods should be abandoned in favour of methods such as the structured walk and cell count methods whose properties of aggregation are better understood.

The final conclusion we will draw relates to more substantive questions. Although we have tackled individual and aggregate analysis here, much finer analysis of the fractal dimension of parts of perimeter boundaries is required. With k land uses, there are $\frac{1}{2}k(k+1)$ possible pairwise boundaries to examine separately. Better classification of the fractal shapes of land parcels will not emerge until the common boundary problem is directly broached. This must involve a detailed examination of how such boundaries are formed and how they evolve over time. By explaining the development process, more satisfactory explanations can be given of the way land uses 'stick' to each other to form the whole town. Only by extending the analysis along these lines can conclusive results about the ways in which urban morphologies are structured and evolve, be demonstrated.

References

- Aviles C A, Scholz C H, Boatwright J, 1987, "Fractal analysis applied to characteristic segments of the San Andreas Fault" *Journal of Geophysical Research* 92 331-344
 Batty M, Longley P A, 1987a, "Fractal-based description of urban form" *Environment and Planning B: Planning and Design* 14 123-134
 Batty M, Longley P A, 1987b, "Urban shapes as fractals" *Area* 19 215-221

- Bracken I, Holdstock S, Martin D, 1987, "MapManager: intelligent software for the display of spatial information", Report 3, Wales and South West Regional Research Laboratory, University of Wales at Cardiff, Cardiff
- Clark N N, 1986, "Three techniques for implementing digital fractal analysis of particle shape" *Powder Technology* 46 45-52
- Goodchild M F, 1980, "Fractals and the accuracy of geographical measures" *Mathematical Geology* 12 85-98
- Goodchild M F, Mark D M, 1987, "The fractal nature of geographic phenomena" *Annals of the Association of American Geographers* 77 265-278
- Gould S J, 1966, "Allometry and size in ontogeny and phylogeny" *Biological Review* 41 587-640
- Kaproff J, 1986, "The geometry of coastlines: a study in fractals", in *Computers and Mathematics with Applications* 12B 651-671; also reprinted in *Symmetry: Unifying Human Understanding* Ed. K Hargittai (Pergamon Press, Oxford) pp 655-671
- Kaye B H, 1978, "Specification of the ruggedness and/or texture of a fineparticle profile by its fractal dimension" *Powder Technology* 21 1-16
- Kaye B H, 1986, "The description of two-dimensional rugged boundaries in fineparticle science by means of fractal dimensions" *Powder Technology* 46 245-254
- Kaye B H, Clark G G, 1985, "Fractal description of extra-terrestrial fineparticles", Department of Physics, Laurentian University, Sudbury, Ontario
- Kaye B H, Leblanc J E, Abbot P, 1985, "Fractal description of the structure of fresh and eroded aluminium shot fineparticles" *Particle Characterization* 2 56-61
- Longley P A, Batty M, 1986, "Measuring and simulating the structure and form of cartographic lines", UWIST Papers in Planning Research 102, Department of Town Planning, University of Wales at Cardiff, Cardiff
- Lovejoy S, 1982, "Area-perimeter relation for rain and cloud areas" *Science* 216 185-187
- Mandelbrot B B, 1977, "Stochastic models for the earth's relief, the shape and the fractal dimension of the coastlines and the number-area rule for islands" *Proceedings of the National Academy of Sciences USA* 72 3825-3828
- Mandelbrot B B, 1983 *The Fractal Geometry of Nature* (W H Freeman, San Francisco, CA)
- Mark D M, Aronson P B, 1984, "Scale-dependent fractal dimensions of topographic surfaces: an empirical investigation, with applications in geomorphology and computer mapping" *Mathematical Geology* 16 671-683
- Muller J C, 1987, "Fractal and automated line generalization" *The Cartographic Journal* 24 27-34
- Orford J D, Whalley W B, 1983, "The use of the fractal dimension to quantify the morphology of irregular-shaped particles" *Sedimentology* 30 655-668
- Richardson L F, 1961, "The problem of contiguity: an appendix to 'Statistics of deadly quarrels'" *General Systems Yearbook* 6 139-187
- Rickaby P, 1987, "An approach to the assessment of the energy efficiency of urban built form", in *Energy and Urban Built Form* Eds D Hawkes, J Owers, P Rickaby, P Steadman (Butterworth, Sevenoaks, Kent) pp 43-61
- Shelby M C, Moellering H, Lam N, 1982, "Measuring the fractal dimensions of empirical cartographic curves" *Auto-Carto* 5 481-490
- Suzuki M, 1984, "Finite size scaling for transient similarity and fractals" *Progress of Theoretical Physics* 71 1379-1400
- Woronow A, 1981, "Morphometric consistency with the Hausdorff-Besicovitch dimension" *Mathematical Geology* 13 201-216